Article

Effect of Metal Carbides on Hydrogen Embrittlement on Steel: A DFT Study

OMAR FAYE * and Jerzy Antony Szpunar

Posted Date: 12 February 2024

doi: 10.20944/preprints202402.0655.v1

Keywords: hydrogen; embrittlement; niobium carbide; titanium carbide; vanadium carbide; manganese sulfide

Article

Effect of Metal Carbides on Hydrogen Embrittlement: A DFT Study

Omar Faye * and Jerzy A. Szpunar

Department of Mechanical Engineering, College of Engineering, University of Saskatchewan,
57 Campus Drive, Saskatoon, SK S7N 5A9, Canada
* Correspondence: omf071@usask.ca or omsofaye@yahoo.fr

Abstract: This study reports the effect of some metal carbide (niobium carbide, vanadium carbide, titanium carbide, and manganese sulfide) on hydrogen embrittlement in pipeline industry using plane wave density functional theory (DFT). Our results predicted that the interaction of hydrogen molecule with these metals carbide occurs in the long range with a binding energy varying in the energy window [0.043 eV to 0.70 eV]. In addition, our study shows the desorption of H_2 molecule from these metals carbides in the chemisorptions. Since, hydrogen embrittlement, occurs in the atomic state of hydrogen, therefore our finding in the atomic interaction of hydrogen with NbC, VC, TiC, and MnS showed that the strength of the trapping of hydrogen atom can be classified as: TiC+H>VC+H>NbC+H> MnS+H. In addition, our study reveals that the carbon site is the most favorable hydrogen trapping site than the metal one.

Keywords: hydrogen; embrittlement; niobium carbide; titanium carbide; vanadium carbide; manganese sulfide

1. Introduction

It is well known that high-strength steels are embrittled in a hydrogenous gaze environment [1–3]. The key factors that favor hydrogen embrittlement are: (i) the dissociation of hydrogen molecule, (ii) the diffusion of hydrogen atom through the pipe, or lattice along a preferential path as the grain boundaries, or dislocation inducing in plastic deformation at critical sites [4]. In addition, embrittlement of the material is enhanced by the decohesion of the atomic layers at the interface, or the recombination of hydrogen atom at the internal voids or defects [5]. Finally, the decrease of the surface energy because of the adsorbed hydrogen or the hydride formation with certain alloys of vanadium, niobium, titanium and zirconium [5]. Therefore, to minimize the effect of hydrogen embrittlement in steel, many theories that lead to this embrittlement are discussed in the literature [6]. It is reported that defect such as dislocations, grain boundaries and inclusion scan be used to alter the hydrogen diffusion into the materials by trapping hydrogen at these defects sites [1]. It is also reported that using secondary phase particles as a trapping site can be an efficient way to improve the mechanical properties by reducing the amount of diffusible hydrogen within the material [7]. Therefore, to promote the competitiveness of steel in the market, high –strength steels have been introduced to guaranty the resistance again hydrogen embrittlement, and stress corrosion cracking in the steel applications. In addition, to avoid the risk of deterioration in material strength, various research have pointed the used of carbide precipitates formed above 500 °C can be a feasible way to maintain the high strength of the steel even after applying a tempering process as reported in the literature [6,8,9].

It is stated that carbide precipitated phase as a hydrogen trap can enhance the resistance to hydrogen embrittlement and generated more secondary cracks at the grain boundary [10,11].

Therefore, a well-designed hydrogen trapping sites can improve the resistance against embrittlement (HE). In addition, it is well know that a limit quantity of hydrogen diffusion may be sufficient to provoke a failure. In the same trend, numerous studies have found that the addition of micro alloying elements (Nb, Ti, V and Mo) might improve the HE resistance of steel [12]. In, addition, metal carbide (MC) nanoprecipitates not only optimize the microstructure and improve the mechanical properties but also increase the hydrogen trap density in the high-strength martensitic steels to improve HE resistance [16].

Buono et la. [12] studied the effect of nano NbC and VC carbides on the hydrogen interaction in tempered martensitic steels. They reported that the trapping capacity decreases in the following order: NbC> TiC>VC>MnS. Based on the existing research, this work aims to investigate the effects of metal carbides nanoprecipitates on the hydrogen embrittlement resistance of high-strength martensitic steels. Firstly, we study the interaction of hydrogen molecule with the bulk structure of these metals.

Secondly, the interaction of hydrogen atom and its preferential adsorption site will be investigated.

Finally, the effect of layers of these carbides on hydrogen embrittlement will be probed.

2. Computational Method

To model, the hydrogen interaction with some metal carbide such as niobium carbide (NbC), titanium carbide (TiC), and vanadium carbide (VC), we use Dmol^3 module implemented in material studio software [13,14]. To approximate the exchange correlation effect of electron- electron interaction, the Perdew–Wang exchange and correlation functional (PW91) was used [15]. Furthermore, the effect of core electron as a single effective potential [16] was represented by using the semicore pseudo potentials. The double numerical plus polarization (DNP) was used as a basis set. To include the van der Waals interaction, we used the (DFT-D) scheme of Grimme et al. [17] [18]. We use 225 as a space group number to model TiC, and VC where Ti and V atoms occupy the origin positions (0, 0, 0), and C atoms are located in (1/2, 0, 0) position. NbC, was also modeled with a space group number of 229 where Nb atoms occupy the origin positions (0, 0, 0) and C atoms are located in (1/2, 0, 0) position. The Brillouin zone integration was performed through the Monkhorst–Pack scheme [47] with a mesh grid of 2×2× 2. The energy minimization was performed with an energy convergence tolerance of 10^{-5} Ha. All atomic positions were relaxed such that the force on each atom was less than 0.002 Ha/Å. To improve the convergence, we use 0.25Ha as a thermal smearing value.

3. Results and Discussion

3.1. Hydrogen Interaction with NbC,TiC, VC and MnS Structure

Hydrogen embrittlement is a serious issue in the pipeline industry. Therefore, to mitigate this issue many researchers are using transition metal carbides as an alternative. In this study, we use niobium carbide (NbC), Titanium carbide (TiC), Vanadium carbide (VC) and Manganese sulfide (MnS) to investigate their effect in the hydrogen embrittlement. To begin with, we display the bulk structure of the under investigated metals carbide in Figure 1.

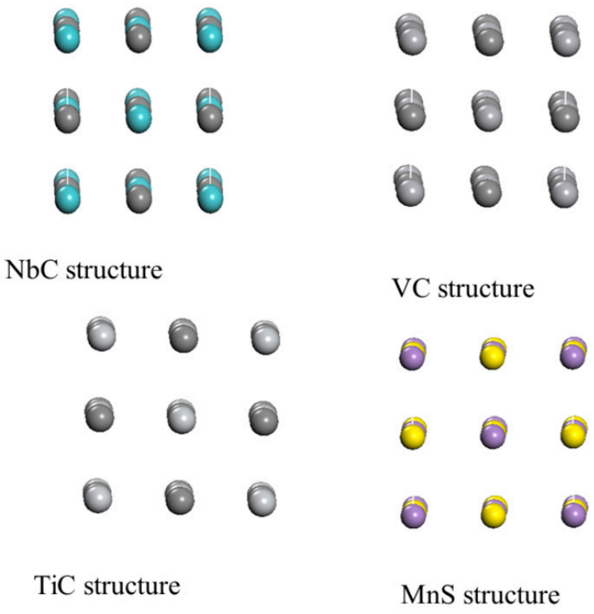

Figure 1. Schematic representation of niobium carbide, Vanadium carbide, Titanium carbide and manganese sulfide. The green balls stand for niobium atoms (Nb), the gray ones stand for carbons (C), the slight gray stand for vanadium (V) and the light gray stand for titanium atoms (Ti), the yellow atoms stand for sulfide, and the purple ones stand for manganese atom (Mn).

The calculated bulk properties such as: the lattice parameter, the band gap energy are listed in Table 1.

Table 1. Lattice parameter and band gap energy of niobium carbide, vanadium carbide, titanium carbide and manganese sulfide.

Metal carbides	Lattice parameter (Å)	Energy band gap E_g(eV)
NbC	4.40	0.006
VC	4.18	0.007
TiC	4.36	0.09
MnS	5.70	3.2

Table1 showed that the calculated lattice parameter of niobium carbide (NbC) is 4.40 Å compared to 4.51 Å [19], and 4.43 [20,21] as reported in the literature. Also, as indicated in Table 1, the calculated lattice parameter of vanadium carbide is 4.180 Å compared the experimental value of 4.16Å [22,23], and the calculated lattice parameter of titanium carbide is 4.36Å compared to its experimental value of 4.32 Å [24–26]. Finally, the calculated lattice parameter and manganese sulfide is 5.07 Å compared to its experimental value of 5.60 Å [27]. The good agreement between the theoretical and experimental value, and also, the small deviation between the experimental and theoretical values showed that our approximation to model these structures is reliable. Furthermore, we study the chemical stability of these metal carbides by determining the energy band gap using equation 2.

$$E_g = E_{LUMO} - E_{HOMO} \tag{1}$$

where E_{LUMO} is the energy of the lowest unoccupied molecular orbital (LUMO), and E_{HOMO} is the energy of the highest occupied molecular orbital (HOMO).

Vacuum space of 15 Å was created in order to avoid the images interaction and to model accurate the adsorption of the metal carbides with hydrogen.

The calculated energy band gap of niobium carbide crystal is 0.04 eV, which is slightly deviated from the zero gap as reported by Delgado et al. [28]. In the same trend, Lin et al. [29] stated that the

doi:10.20944/preprints202402.0655.v1

vanadium carbide has good metal properties, which is in good agreement with our energy band gap calculation (E_g) of 0.007eV. Also, Mohsen et.al [24] predicted similar characteristic for titanium carbide for a zero band gap energy compared to our computed value of 0.09eV. In contrast with manganese sulfide (MnS) where the experimental value the energy band gap is 3 eV [27,30] compared to our calculated value of 3.2 eV.

Moreover, knowing their lattice parameter and their chemical stability, we further study the most two common ways that molecular hydrogen interacts with those metal carbides (physisorption and chemisorptions).

Firstly, we study the interaction of hydrogen molecule in the physisorption case with niobium carbide (NbC), titanium carbide (TiC), vanadium carbide (VC) and manganese sulfide (MnS). The initial and optimized structures in the physisorption interaction of hydrogen with these metal carbides are shown in Figure 2.

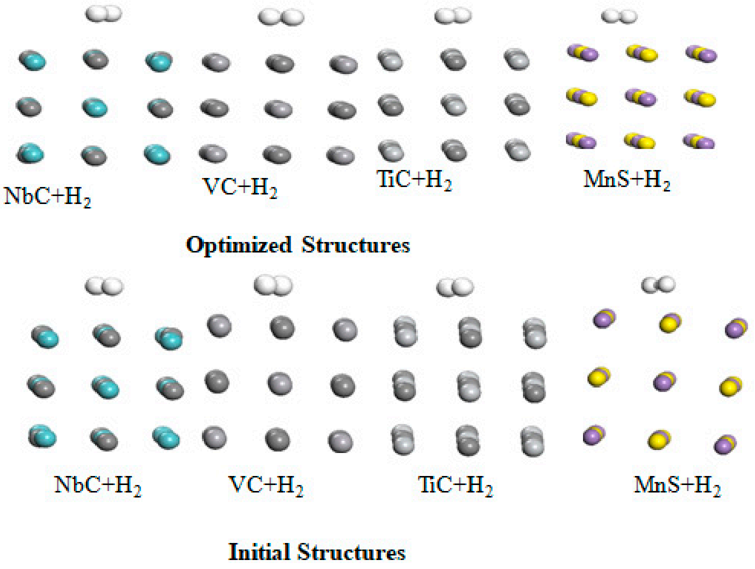

Figure 2. The initial and final structure of the interaction of hydrogen molecule with NbC, TiC, VC, and MnS. The green balls stand for niobium atoms (Nb), the gray ones stand for carbons (C), the slight gray stand for vanadium (V) and the light gray stand for titanium atoms (Ti), the yellow atoms stand for sulfide, the white balls stand for hydrogen atom (H), and the purple ones stand for manganese atom (Mn).

To do so, we evaluate the strength of the interaction of H_2 molecule with those metal carbides we use the equation (2):

$$E_b = E_{(MC)} + E_{(H)} - E_{(MC+H)} \qquad (2)$$

where $E_{(MC)}$ stands for the total energy of the metal carbide in it primitive unit cell, $E_{(H)}$ the ground energy of hydrogen molecule in a cubic cell of lattice parameter (a=20 Å) or, and $E_{(MC+H)}$ the total energy of the metal carbide plus the H_2 molecule.

The calculated binding energy along with their equilibrium distance of these optimized structures are summarized in Table 2.

Table 2. Adsorption energy of hydrogen molecule with niobium carbide, titanium carbide, vanadium carbide and manganese carbide.

Metal carbide +H_2 molecule	Adsorption energy E_b(eV)	d_{eq}(Å)
NbC+H_2	0.050	1.417
TiC+H_2	0.70	1.204
VC+H_2	0.62	1.309
MnS+H_2	0.043	1.810

Table 2 revealed that the binding energy between hydrogen molecule and these metal carbides in the physisorption case are the wan der Waal interaction, where the adsorption energy ranging from 0.043 eV to 0.70 eV. In addition, their equilibrium distance falls in the range 1.204 Å to 1.810 Å, which are determined from their optimize structure as displayed in Figure 2. These calculated results align with the earlier results reported in the literature [1,31,32].

Furthermore, we investigate the interaction of hydrogen with the precipitate in the presence steel. To do so, Fe crystal was cleaved along {111}, {110}, and {100} surfaces. After calculation, Fe {110} surface was identified to have the most stabilization compared to other Fe surfaces. Therefore, Fe{110} surface was selected to study the interaction of hydrogen molecules sandwiched between the Fe{110} surface and the four precipitates (NbC, TiC, VC, and MnS). The initial and optimized structures of this interaction are displayed on Figure 3.

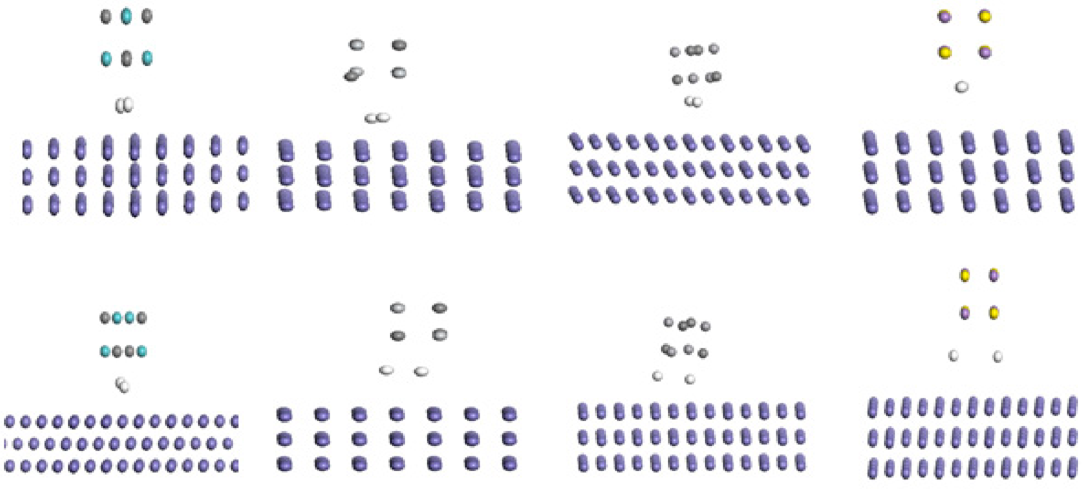

Figure 3. The initial and final structure of the interaction of hydrogen molecule sandwiched between Fe{110} surface, and NbC, TiC, VC, and MnS. The green balls stand for niobium atoms (Nb), the gray ones stand for carbons (C), the slight gray stand for vanadium (V) and the light gray stand for titanium atoms (Ti), the yellow atoms stand for sulfide, the white balls stand for hydrogen atom (H), and the purple ones stand for manganese atom (Mn).

Figure 3 reveals total dissociation of H_2 molecule in all cases. The binding energy, and the equilibrium distance of H_2 between Fe {110}, and the precipitates are summarized in Table 3. Initially we placed H_2 molecule at a distance of 2.6 Å with respect the Fe{110} and 2.8Å with respect the precipitate atom.

Table 3. Summarize the equilibrium parameters such as binding energy (E_b(eV)), and the optimized distance of hydrogen atom with respect the Fe atom and H atom (d_{eq}(Å)).

Fe(110)+Metal carbide +H_2 molecule	Adsorption energy E_b(eV)	d_{eq}(Å)	d_{eq}(Å)
Fe(110)+NbC+H_2	0.320	2.63	2.38
Fe(110)+TiC+H_2	0.570	3.64	2.42
Fe(110)+VC+H_2	0.42	2.68	2.52
Fe(110)+MnS+H_2	0.13	3.21	2.89

The equilibrium distance between the hydrogen atom and the closest top atoms of Fe{110} surface fall in the interval [2.6 to 3.21Å], while [2.38 to 2.65Å] in the cases of the precipitates as shown Table 3. From our results, we can state that the presence of Fe surface favors the dissociation of H_2 molecule. Also, the dissociated hydrogen atoms are closer to the precipitate atoms than the Fe{110} surface.

Furthermore, the interaction of H_2 in the chemisorptions case with the aforementioned metal carbides was investigated. Their initial and optimized structures of these complexes are portrayed in Figure 4 to better visualize this interaction.

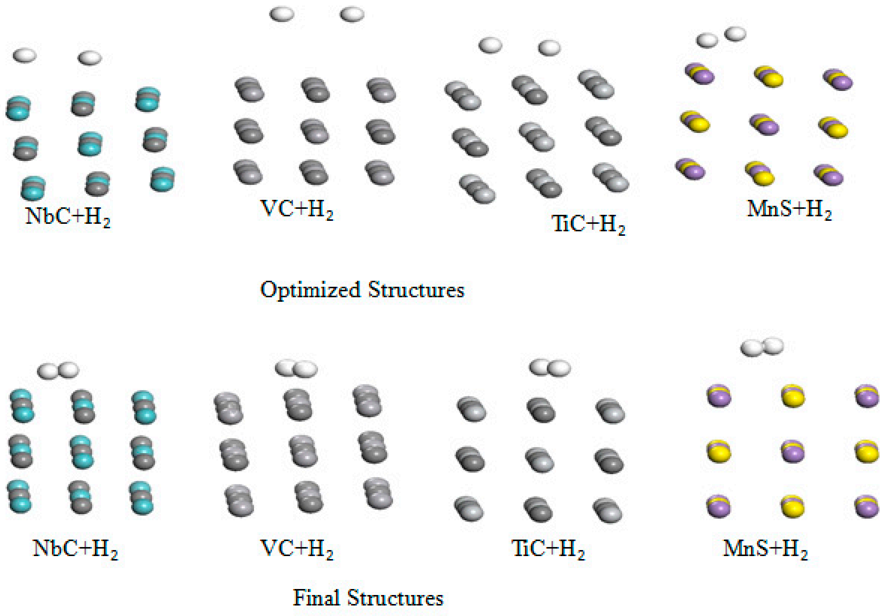

Figure 4. Initial and optimized structures of niobium carbide (NbC), Titanium carbide (TiC), Vanadium carbide (VC) and Manganese sulfide (MnS). The green balls stand for niobium atoms (Nb), the gray ones stand or carbons (C), the slight gray stand for vanadium (V) and the light gray stand for titanium atoms (Ti), the yellow atoms stand for sulfide, the white balls stand for hydrogen atom (H), and the purple ones stand for manganese atom (Mn).

Our calculations reveal spontaneous dissociation of H_2 molecule occurs in all cases in the chemisorptions of hydrogen with these metals carbides as shown in Figure 3. This result aligns with the earlier result of Silveri et al. [31], where, they showed a spontaneous dissociative chemisorption was observed to happen when the molecule was placed less than 2.0 Å above the topmost surface atomic plane. To better visualize these results, we summarized the equilibrium parameters such as binding energy (E_b), and the optimized distance of hydrogen with the matrix (d_{eq}) are summarized in Table 4.

Table 4. Summarized the final parameters such as: binding energy (E_b) and equilibrium distance (d_{eq}).

Metal carbide	Adsorption energy E_b(eV)	d_{eq}(Å)
NbC	039eV	2.04
VC	0.59eV	1.867
TiC	0.63eV	1.678
MnS	0.46eV	1.89

From Table 4, the strength of the hydrogen trapping can be arranged in the following order: TiC+H_2 >VC+H_2>MnS+H_2> NbC+H_2 and the equilibrium distance varies in this interval [1.67 Å to 2.04 Å]. According to the literature, the trapping of hydrogen can be generally classified as strong or weak. Weak trapping occurs when the binding energy is less than 0.31eV (30 KJ mol) while a strong trapping happens when the trapping energy is greater than 0.63eV (60 KJ/mol) [1]. These results predict that all these metal carbides with their binding energy with hydrogen molecule are greater than 0.63 eV is irreversible. Therefore, NbC, TiC and VC are potential precipitates to enhance the strength of the steel due to their strong hydrogen trapping energy. Since, the hydrogen embrittlement occurs essential in the atom state of hydrogen. Therefore, in the next section, we investigate the interaction of hydrogen atom with those metals carbides.

3.2. Interaction of the Metal Carbide (NbC, TiC, VC, and MnS) with Hydrogen Atom

Since, the hydrogen can interact with metal from two types of sources: hydrogen generate at the metal surface and the gaseous hydrogen. At gaseous state, it is in the molecular form at standard conditions, therefore it does not produce embrittlement. However, the atomic hydrogen creates embrittlement due to the fact that atomic hydrogen dissolves rapidly into the metal at room temperature [33]. Therefore, to have more insight in the hydrogen embrittlement on these carbides, we propose to investigate the interaction of hydrogen atom with these metal carbides. To do so we created two layers of bulk crystal separate by a vacuum of 15 Å and 15 Å vacuum or the top layer in order to avoid the strong interaction between these layers.

We display the initial and optimized structures of this interaction in Figure 5.

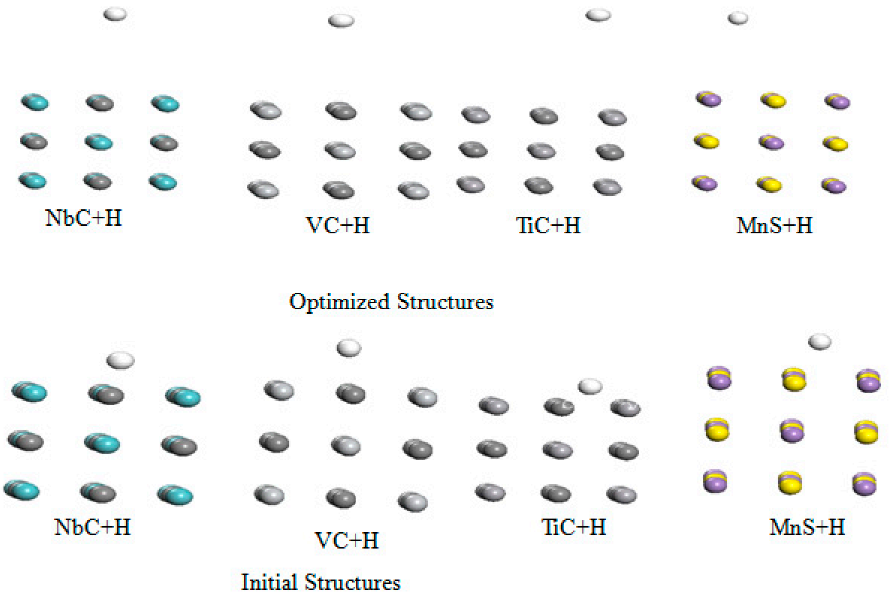

Figure 5. Representation of the initial and final structures of the interaction of hydrogen atom with NbC, VC, TiC and MnS.

doi:10.20944/preprints202402.0655.v1

From these optimized structures, we summarize their optimized parameters such as binding energy (E_b) and final distance between hydrogen atom and these metal carbides (d_{eq}) on Table 5.

Table 5. Summarized the adsorption energy and the optimized distance o hydrogen with NbC, VC, TiC and MnS.

Metal carbide +H_2 molecule	**Adsorption energy E_b(eV)**	**d_{eq}(Å)**
NbC+H	0.240	1.94
VC+H	0.48	1.78
TiC+H	0.840	1.13
MnS+H	0.127	2.08

Table 5 reveals that the most favorable trap site for hydrogen atom among these metal carbides are the TiC with E_b=0.840 eV, VC with E_b=0.480 eV, NbC with E_b=0.240 eV, and MnS with E_b=0.127 eV. In addition, their corresponding equilibrium distance (d_{eq}) ranges in the interval [1.13 Å, 2.08 Å]. Moreover, we study the most favorable adsorption site between the metal and the carbon atom in these metal carbides. To do so, we chemisorbed the hydrogen atom on the carbon and metal site successively, and determine the binding energy on these sites using equation 1.

The adsorption energy (E_b), and their corresponding final distance (d_f) of hydrogen atom with these metal carbide are summarized in Table 6.

Table 6. Summarized the optimized parameters such as binding energy and the final distance between hydrogen atom and the adsorption site.

Metal carbides	**Adsorption energy site**	**Adsorption energy (eV)**	**final distance (d_f) (Å)**
NbC	C	1.22	1.14
	Nb	0.96	1.50
VC	C	1.33	1.14
	V	1.03	1.29
TiC	C	1.55	1.14
	Ti	1.04	1.862
MnS	Mn	0.88	1.73
	S	1.28	1.65

From Table 6, we learnt that the most favorable adsorption site is the carbon site in NbC, VC and TiC with a binding energy lying in the energy window [1.22 eV, 1.55 eV]. While the binding energy of the metal site (Nb, V, and Ti) varying in this interval [0.96 eV, 1.04 eV]. However, for manganese sulfide (MnS) the most favorable trapping site is the sulfur atom with E_b = 1.28 eV compared to E_b= 0.88 eV for the manganese atom (Mn). The trend of this results follows the earlier results reported in the literature [31]. The last section, will discuss the effect of layer on the trapping capacity of the carbides.

3.3. The Effect Layer on Hydrogen Interaction with NbC, TiC, and VC

Understanding the interaction of H_2 molecule and hydrogen atom help us to find new direction of research. In this section we investigate the effect layer on the hydrogen embrittlement on niobium carbide, Titanium carbide, and Vanadium carbide and manganese sulfide. Firstly, we use two layers with a vacuum spacing of 15 Å. The initial and optimize structures of these metals carbides are showed in Figure 6 below.

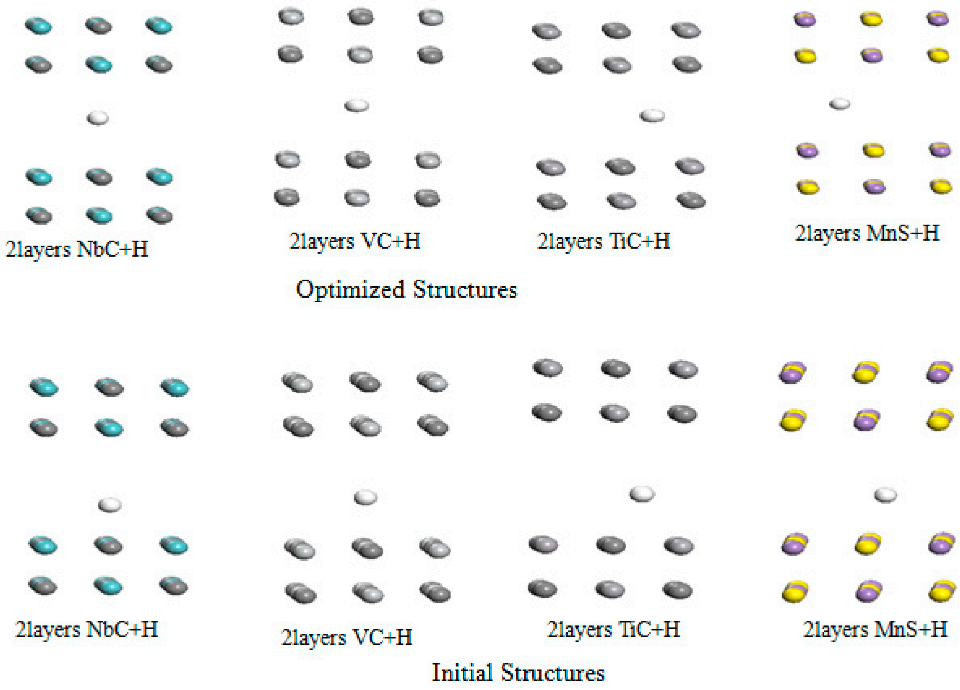

Figure 6. displays the initial and optimized structures niobium carbide, Titanium carbide, Vanadium carbide and Manganese Sulfide.

Furthermore, we determine the strength of the interaction of hydrogen atom with the two layers of NbC, TiC, VC, and MnS using equation (2).

The optimized parameters such as: binding energy of hydrogen atom with those metals carbides are summarized in Table 7.

Table 7. Summarized the adsorption energy of NbC, VC, TiC and MnS along the energy band.

Metal carbide	Adsorption energy E_b(eV)	d_{eq}(Å)
NbC	0.34	1.65
VC	0.52	1.45
TiC	0.88	1.24
MnS	0.21	1.76

Table 7 reveals that the adsorption energy is in the energy window 0.21 to 0.88 eV. The binding of H atom is more favorable in the case of NbC layer. In addition, their optimized distance is between 1.24 Å to 1.76 Å. We notice a slight increase in the binding energy of hydrogen atom in these carbides. Furthermore, we increase the number of layer from two to three for all carbides. The initial and optimized structures in this interaction are shown Figure 7.

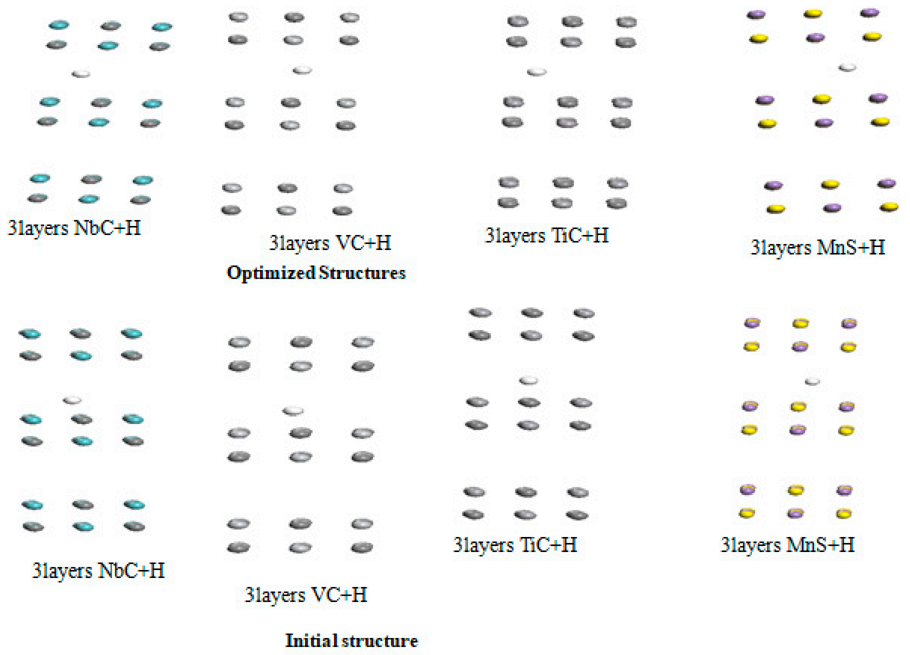

Figure 7. Initial and optimized structures of the interaction of hydrogen with three layers of bulk NbC, VC, TiC, and MnS.

Moreover, we summarized in Table 7 the resulting parameters like adsorption energy and equilibrium distance for the interaction between hydrogen atom and the carbides under study.

Table 7. Summarized the adsorption energy of NbC, VC, TiC and MnS along with their equilibrium distance.

Metal carbide	Adsorption energy E_b(eV)	d_{eq}(Å)
2NbC +H	0.34	1.78
2VC+H	0.56	1.45
2TiC+H	0.93	1.32
2MnS+H	0.28	1.87

From Table 7, we notice that the adsorption energy increases by increasing the number of layers. These results prove that increasing the layer of these carbides can also be an efficient way to enhance the trapping of hydrogen on these carbides.

4. Conclusions

We use plane-wave density functional theory to study the hydrogen interaction with some metals carbide such as: Niobium carbide (NbC), Titanium carbide (TiC), Vanadium carbide (VC) and manganese sulfide (MnS). Our results suggest that the interaction of molecule hydrogen with these metal carbides happen in the gas phase with a binding energy in the energy window [0.70 eV to 0.043 eV]. Also, our results predicted that H_2 desorbed from these metal in case of chemisorptions. Since, hydrogen embrittlement, occurs in the atomic state of hydrogen, therefore our finding in the atomic interaction of hydrogen with NbC, VC, TiC, and MnS showed that the strength of the trapping of hydrogen atom can be classified as: TiC+H>VC+H>NbC+H> MnS+H. In addition, our study reveals that the metal site is the most favorable hydrogen trapping site than the carbon one. Furthermore, our results demonstrate also that increasing the layer can also e an efficient way to enhance the trapping capacity.

Author Contributions: I am the main investigator for this research. Professor Jerzy Szpunar is the principal supervisor for this research.

Funding: No funding is not applicable.

Data Availability Statement: Data will be made available on request.

Acknowledgments: We acknowledge access to high-performance supercomputers, Compute Canada, and Plato at the University of Saskatchewan. This work was supported by the National Engineering Research Council of Canada and the Canada Research Chairs program.

Conflicts of Interest: The authors declare no competing financial interest.

References

1. R. Salehin, G.B. Thompson, C.R. Weinberger, Hydrogen trapping and storage in the group IVB-VIB transition metal carbides, Mater. Des. 214 (2022). https://doi.org/10.1016/j.matdes.2022.110399.
2. M. Wasim, M.B. Djukic, Hydrogen embrittlement of low carbon structural steel at macro-, micro- and nano-levels, Int. J. Hydrogen Energy. 45 (2020) 2145–2156. https://doi.org/10.1016/j.ijhydene.2019.11.070.
3. X. Zhou, A. Tehranchi, W.A. Curtin, Mechanism and Prediction of Hydrogen Embrittlement in fcc Stainless Steels and High Entropy Alloys, Phys. Rev. Lett. 127 (2021). https://doi.org/10.1103/PhysRevLett.127.175501.
4. M. Neikter, M. Colliander, C. de Andrade Schwerz, T. Hansson, P. Åkerfeldt, R. Pederson, M.L. Antti, Fatigue crack growth of electron beam melted TI-6AL-4V in high-pressure hydrogen, Materials (Basel). 13 (2020). https://doi.org/10.3390/ma13061287.
5. M.K. Schaper, Fatigue crack closure at near-threshold growth rates in steels, effects of microstructure, load sequence and environmen, J. ASTM Int. 9 (2012). https://doi.org/10.1520/JAI103968.
6. Y. Wang, X. Wang, J. Gong, L. Shen, W. Dong, Hydrogen embrittlement of catholically hydrogen-precharged 304L austenitic stainless steel: Effect of plastic pre-strain, in: Int. J. Hydrogen Energy, 2014: pp. 13909–13918. https://doi.org/10.1016/j.ijhydene.2014.04.122.
7. A. Nagao, M.L. Martin, M. Dadfarnia, P. Sofronis, I.M. Robertson, The effect of nanosized (Ti,Mo)C precipitates on hydrogen embrittlement of tempered lath martensitic steel, Acta Mater. 74 (2014) 244–254. https://doi.org/10.1016/j.actamat.2014.04.051.
8. L.B. Peral, A. Zafra, I. Fernández-Pariente, C. Rodríguez, J. Belzunce, Effect of internal hydrogen on the tensile properties of different CrMo(V) steel grades: Influence of vanadium addition on hydrogen trapping and diffusion, Int. J. Hydrogen Energy. 45 (2020) 22054–22079. https://doi.org/10.1016/j.ijhydene.2020.05.228.
9. L.B. Peral, I. Fernández-Pariente, C. Colombo, C. Rodríguez, J. Belzunce, The positive role of nanometric molybdenum–vanadium carbides in mitigating hydrogen embrittlement in structural steels, Materials (Basel). 14 (2021). https://doi.org/10.3390/ma14237269.
10. T. Depover, K. Verbeken, The effect of TiC on the hydrogen induced ductility loss and trapping behavior of Fe-C-Ti alloys, Corros. Sci. 112 (2016) 308–326. https://doi.org/10.1016/j.corsci.2016.07.013.
11. S.K. Lawrence, J.P. Wharry, Hydrogen Effects on Material Performance, JOM. 72 (2020) 1979–1981. https://doi.org/10.1007/s11837-020-04123-6.
12. T.A.A. dos Santos, M.M. de Lima, D.S. dos Santos, V.T.L. Buono, Effect of nano Nb and V carbides on the hydrogen interaction in tempered martensitic steels, Int. J. Hydrogen Energy. 47 (2022) 1358–1370. https://doi.org/10.1016/j.ijhydene.2021.10.051.
13. B. Delley, From molecules to solids with the DMol3 approach, J. Chem. Phys. 113 (2000) 7756–7764. https://doi.org/10.1063/1.1316015.
14. ...Materials Studio, Chem. Eng. News Arch. 78 (2000) ibc. https://doi.org/10.1021/cen-v078n013.ibc.
15. J.P. Perdew, K. Burke, M. Ernzerhof, Generalized gradient approximation made simple, Phys. Rev. Lett. 77 (1996) 3865–3868. https://doi.org/10.1103/PhysRevLett.77.3865.
16. J.P. Perdew, J.A. Chevary, S.H. Vosko, K.A. Jackson, M.R. Pederson, D.J. Singh, C. Fiolhais, Applications of the generalized gradient approximation for exchange and correlation, Phys Rev B. 46 (1992) 6671--. http://link.aps.org/abstract/PRB/v46/p6671.
17. S. Grimme, J. Antony, S. Ehrlich, H. Krieg, A consistent and accurate ab initio parametrization of density functional dispersion correction (DFT-D) for the 94 elements H-Pu, J. Chem. Phys. 132 (2010). https://doi.org/10.1063/1.3382344.
18. O. Faye, U. Eduok, J.A. Szpunar, Boron-Decorated Graphitic Carbon Nitride (g-C3N4): An Efficient Sensor for H2S, SO2, and NH3 Capture, J. Phys. Chem. C. 123 (2019) 29513–29523. https://doi.org/10.1021/acs.jpcc.9b06032.
19. D. Connétable, First-principles study of transition metal carbides, Mater. Res. Express. 3 (2016). https://doi.org/10.1088/2053-1591/3/12/126502.

20. H.W. Hugosson, U. Jansson, B. Johansson, O. Eriksson, Phase stability diagrams of transition metal carbides, a theoretical study, Chem. Phys. Lett. 333 (2001) 444–450. https://doi.org/10.1016/S0009-2614(00)01414-7.
21. S. Sun, H. Fu, J. Lin, G. Guo, Y. Lei, R. Wang, The stability, mechanical properties, electronic structures and thermodynamic properties of (Ti, Nb)C compounds by first-principles calculations, J. Mater. Res. 33 (2018) 495–506. https://doi.org/10.1557/jmr.2017.440.
22. F. Liu, Y. Yao, H. Zhang, Y. Kang, G. Yin, Z. Huang, X. Liao, X. Liang, Synthesis and characterization of vanadium carbide nanoparticles by thermal refluxing-derived precursors, J. Mater. Sci. 46 (2011) 3693–3697. https://doi.org/10.1007/s10853-010-5123-y.
23. Y. Liu, S. Huang, J. Ding, Y. Yang, J. Zhao, Vanadium carbide coating as hydrogen permeation barrier: A DFT study, Int. J. Hydrogen Energy. 44 (2019) 6093–6102. https://doi.org/10.1016/j.ijhydene.2019.01.049.
24. M. Mhadhbi, Titanium Carbide: Synthesis, Properties and Applications, Brill. Eng. 2 (2020) 1–11. https://doi.org/10.36937/ben.2021.002.001.
25. H. Xiong, H. Zhang, H. Zhang, L. Gan, First Principle Calculation of NbC Precipitation Competition between TiC Particle and Ferrite Matrix, J. Wuhan Univ. Technol. Mater. Sci. Ed. 33 (2018) 1076–1081. https://doi.org/10.1007/s11595-018-1937-2.
26. Y. Yang, H. Lu, C. Yu, J.M. Chen, First-principles calculations of mechanical properties of TiC and TiN, J. Alloys Compd. 485 (2009) 542–547. https://doi.org/10.1016/j.jallcom.2009.06.023.
27. A. M. Ferretti, S. Mondini, A. Ponti, Manganese Sulfide (MnS) Nanocrystals: Synthesis, Properties, and Applications, in: Adv. Colloid Sci., 2016. https://doi.org/10.5772/65092.
28. N. Delgado, O. Salas, E. Garcés, L.F. Magaña, Ab-Initio Calculation of the Electrical Conductivity, Optical Absorption, and Reflectivity of the 2D Materials SnC and NbC, Crystals. 13 (2023) 1–9. https://doi.org/10.3390/cryst13040682.
29. L. Lin, X. Yang, P. Shi, L. Yan, K. Xie, C. Deng, Z. Chen, Probing the origin of transition metal carbide VC for oxygen reduction reaction: A DFT study, Surfaces and Interfaces. 40 (2023) 103100. https://doi.org/10.1016/j.surfin.2023.103100.
30. Hansa, S. Sahani, T.Y. Kim, Metal Nanocomposites for Energy and Environmental Applications, in: Energy, Environ. Sustain., 2022: pp. 293–318. https://doi.org/10.1007/978-981-16-8599-6_13.
31. F. Silveri, M.G. Quesne, A. Roldan, N.H. De Leeuw, C.R.A. Catlow, Hydrogen adsorption on transition metal carbides: A DFT study, Phys. Chem. Chem. Phys. 21 (2019) 5335–5343. https://doi.org/10.1039/c8cp05975f.
32. L. Vandewalle, T. Depover, K. Verbeken, Hydrogen trapping of carbides during high temperature gaseous hydrogenation, Int. J. Hydrogen Energy. (2023). https://doi.org/10.1016/j.ijhydene.2023.04.348.
33. J. Song, W.A. Curtin, Atomic mechanism and prediction of hydrogen embrittlement in iron, Nat. Mater. 12 (2013) 145–151. https://doi.org/10.1038/nmat3479.